

# Computational Imaging Using Deterministic Optical Fields and Non-linear Reconstruction

Francis Gracy Arockiaraj,<sup>1</sup> Shakina Jothi Selva,<sup>1</sup> Stephen Rajkumar Inbanathan,<sup>1</sup> Manueldoss Beaula Ruby Kamalam,<sup>1</sup> Aravind Simon John Francis Rajeswary,<sup>2</sup> Vijayakumar Anand,<sup>2,3,\*</sup> and Joseph Rosen<sup>4</sup>

<sup>1</sup>PG & Research Department of Physics, The American College, Madurai, 625 002, Tamilnadu, India.

<sup>2</sup>Institute of Physics, University of Tartu, 50411 Tartu, Estonia.

<sup>3</sup>Optical Sciences Center and ARC Training Centre in Surface Engineering for Advanced Materials (SEAM), Swinburne University of Technology, Hawthorn, Melbourne, Victoria 3122, Australia.

<sup>4</sup>School of Electrical and Computer Engineering, Ben Gurion University of the Negev, P. O. Box 653, 8410501, Israel.

[vijayakumar.anand@ut.ee](mailto:vijayakumar.anand@ut.ee)

**Abstract:** Computational imaging techniques are indirect ones consisting of two steps: optical recording and computational reconstruction. In this study, deterministic optical fields such as Bessel, Airy, Gaussian and Laguerre-Gaussian were studied in this indirect imaging framework. © 2022 The Author(s)

## 1. Introduction

Computational imaging techniques (CITs), in general, involve two steps: optical recording and computational reconstruction [1]. The CITs that use linear shift-invariant (LSI) systems with spatially incoherent and temporally coherent illumination can be completely characterized by measuring the point spread function (PSF). The optical configuration of CITs consists of three main components, namely object, optical modulator and image sensor. The light from every point of an object is transformed by the optical modulator into an intensity distribution at the sensor plane. In past studies, special coded apertures such as uniformly redundant array (URA) [2], modified URA [3] and chaotic coded apertures [4] have been widely used. The choice of the mask pattern depends upon the computational reconstruction method. In 2018, a computational reconstruction method called the non-linear reconstruction (NLR) was developed for CITs involving chaotic coded apertures [5], which was found to be highly efficient. Later, it was found that NLR is also effective for optical fields such as Bessel [6], double helix beams [7] and Cassegrain objective lenses [8] in the indirect imaging framework. All the above beams have been found useful for many applications such as optical trapping, laser ablation, tomography and optical communication. The capability to image using these beams will aid in simplifying the dual-beam setups [1]. There is already a shift in focus in using deterministic optical fields instead of speckle fields for 3D imaging as the photon budget requirements are quite high for the speckle fields. In this study, we have investigated the 3D imaging characteristics of several well-known deterministic optical fields using NLR.

## 2. Methods

The imaging concept is shown in Figure 1(a). Different optical components such as a refractive lens, refractive axicon, spiral phase plate (SPP) and cubic phase mask (CPM) are used to transform a point in the object plane into a point, Bessel, vortex and accelerating Airy beam intensity distributions respectively. The object intensity pattern  $I_O$  obtained for an object  $O$  is given as  $I_O = O \otimes I_{PSF}$ , where  $I_{PSF}$  is the point spread function and  $\otimes$  indicates convolution. In an LSI, by recording the  $I_{PSF}$ , it is possible to reconstruct the object information as  $I_R = I_O * I_{PSF}$ , which can be rewritten, by substituting  $I_O$ , as  $I_R = O \otimes (I_{PSF} * I_{PSF})$ , where  $*$  indicates correlation. Depending upon the sharpness of the autocorrelation function  $I_{PSF} * I_{PSF}$ , the object information is resolved during reconstruction. The sharpness of the autocorrelation function is dependent upon the nature of  $I_{PSF}$  and the type of correlation operation. The NLR approach of the cross-correlation is given as  $|\mathfrak{F}^{-1}\{|O' I_{PSF}'|^{\beta} \exp[i(\phi_O + \phi_{PSF})]\} I_{PSF}'|^{\alpha} \exp[-i(\phi_{PSF})]|$ , where  $O'$  and  $I_{PSF}'$  are the Fourier transforms of  $I_{PSF}$  and  $O$ .  $\mathfrak{F}^{-1}$  is the inverse Fourier transform operator. By tuning  $\alpha$  and  $\beta$  between -1 to +1 it is possible to obtain an improved image with weaker background noise than other filters such as matched filter ( $\alpha = \beta = 1$ ), phase-only filter ( $\alpha = 0, \beta = 1$ ), and inverse filter ( $\alpha = -1, \beta = 1$ ) [5,9].

Two test objects: central parts of emblems of the University of Tartu and Ben Gurion University of the Negev, were used to study the imaging performance for different optical fields using non-linear reconstruction. The simulation has been carried out using matrices of  $500 \times 500$  pixels, with a pixel size of  $10 \mu\text{m}$  and  $\lambda = 600 \text{ nm}$ . The object distance and image distance were set to 40 cm. The simulated PSFs for two transverse planes (separated by a gap of  $\Delta z = 10 \text{ cm}$ ) for the above different cases: lens (focal length = 20 cm), axicon (Period =  $300 \mu\text{m}$ ), SPP with topological charge = 1 multiplexed with a lens and CPM whose phase given as  $\exp\{ik(x^3 + y^3)\}$  with  $k=0.1629$  are

shown in Figs. 1(b). As expected, for lens-based elements such as lens and spiral phase plate multiplexed with lens, the intensity distribution varied with distance, while for non-diffracting beams such as Airy and Bessel beams, the variation is insignificant. The intensity distributions obtained for the two test objects and their corresponding reconstruction results at the two planes using non-linear reconstruction are shown in Figs. 1(b). Fresnel diffraction integral was used for simulation of the optical fields at two different planes [10]. While it is expected that the values of  $\alpha$  and  $\beta$  will be different for different cases, the imaging performance seems to be better for some cases while it is not for others for the optimal conditions. The optimal values of  $\alpha$  and  $\beta$  were 0 and 0.6 for the lens, axicon and spiral phase plate but were 0.3 and 0 and 0.6 and 0 for the accelerating airy beam case.

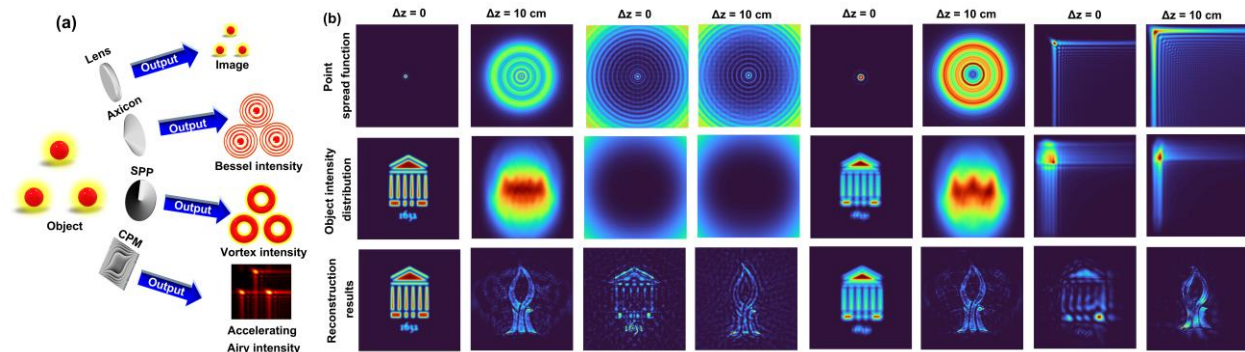


Figure 1. (a) Optical configuration of the CIT. (b) Simulation results of generation of PSF, object intensity distribution of two objects: central part of emblems of the Tartu University and Ben Gurion University of the Negev at two distances  $\Delta z = 0$  and 10 cm for a lens, axicon, SPP with topological charge =1 and CPM. SPP - spiral phase plate, CPM - cubic phase mask.

### 3. Discussion and Conclusion

In the indirect imaging framework, deterministic optical fields generated by a lens, axicon, SPP and a CPM have been investigated for 3D imaging using the NLR method. In most cases, the object information has been successfully reconstructed at the optimal values of  $\alpha$  and  $\beta$ . However, the outcome is not the same for all the cases. We believe that the study will assist in replacing the dual-beam configuration [1] with a single beam in many applications where the application, as well as imaging, may be carried out using the same beam. The current study also reveals that NLR may be a universal reconstruction method for optical encryption applications. The application of deep learning-based noise reduction methods along with NLR may improve the reconstruction results further.

**Acknowledgments** European Union's Horizon 2020 research and innovation programme grant agreement No. 857627 (CIPHR) is acknowledged for funding.

### References

- [1] J. Rosen, A. Vijayakumar, M. Kumar, M. R. Rai, R. Kelner, Y. Kashter, A. Bulbul, and S. Mukherjee, "Recent advances in self-interference incoherent digital holography," *Adv. Opt. Photon.* **11**, 1-66 (2019).
- [2] E. E. Fenimore and T. M. Cannon, "Coded aperture imaging with uniformly redundant arrays," *Appl. Opt.* **17**, 337-347 (1978).
- [3] S. R. Gottesman and E. E. Fenimore, "New family of binary arrays for coded aperture imaging," *Appl. Opt.* **28**, 4344-4352 (1989).
- [4] J. Rosen, *et al.* "Roadmap on chaos-inspired imaging technologies (CI<sup>2</sup>-Tech)," *Appl. Phys. B* **128**, 49 (2022).
- [5] M. R. Rai, A. Vijayakumar, and J. Rosen, "Non-linear adaptive three-dimensional imaging with interferenceless coded aperture correlation holography (I-COACH)," *Opt. Express* **26**, 18143-18154 (2018).
- [6] D. Smith, S. H. Ng, M. Han, T. Katkus, V. Anand, K. Glazebrook and S. Juodkazis, "Imaging with diffractive axicons rapidly milled on sapphire by femtosecond laser ablation," *Appl. Phys. B* **127**, 11 (2021).
- [7] V. Anand, S. Khonina, R. Kumar, N. Dubey, A. N. K. Reddy, J. Rosen and S. Juodkazis, "Three-Dimensional Incoherent Imaging Using Spiral Rotating Point Spread Functions Created by Double-Helix Beams [Invited]," *Nanoscale Res. Lett.* **17**, 37 (2022).
- [8] V. Anand, M. Han, J. Maksimovic, S. H. Ng, T. Katkus, A. Klein, K. Bamberg, M. J. Tobin, J. Vongsivut and S. Juodkazis, "Single-shot mid-infrared incoherent holography using Lucy-Richardson-Rosen algorithm," *Opto-Electron. Sci.* **1**, 210006 (2022).
- [9] A. Vijayakumar, D. Jayavel, M. Muthaiah, S. Bhattacharya, and J. Rosen, "Implementation of a speckle-correlation-based optical lever with extended dynamic range," *Appl. Opt.* **58**, 5982-5988 (2019).
- [10] A. Vijayakumar and S. Bhattacharya, *Design and Fabrication of Diffractive Optical Elements with MATLAB* (SPIE, 2017).